


Silver-iron beads for removal of amoxicillin antibiotic from water using simulated permeable reactive barrier-column study

Dalal Ghanim Yahia¹, Ayad A.H. Faisal^{1*} 

¹ Department of Environmental Engineering, College of Engineering, University of Baghdad, Baghdad, Iraq

* Corresponding author's e-mail: ayad.faisal@coeng.uobaghdad.edu.iq

ABSTRACT

The innovative aspect of this study is synthesis of a novel sorbent (Ag/Fe – nanoparticles – sodium alginate beads) that can be employed for treating simulated groundwater polluted with amoxicillin (AMX) antibiotic in permeable reactive barrier (PRB) – continuous configuration. The beads are prepared using solid residues, especially the peels of pomegranate and leaves of sesban tree, to satisfy the sustainability concepts. The sorbent was prepared through manufacturing of nanoparticles from silver and iron layered double hydroxides and; then, immobilization the nanoparticles with sodium alginate. The particles have been manufactured through mixing silver – iron ions obtained with peels of pomegranate and leaves of sesban tree respectively via precipitation method. The suitable conditions for bead preparation to obtain maximum removal efficiency of AMX are molar ratio (Ag/Fe) = 0.5, solution pH = 9, and silver to iron nanoparticles dosage = 7 g per 100 mL of sodium alginate. The characterization tests of beads prove that nanoparticles can support antibiotic sorption. Results certified that PRB can restrict the migration of AMX and its longevity is correlated directly with the thickness of beads; in addition, it is inversely correlated with inlet concentration and water flowrate. The measurements of continuous tests for removing of AMX have fitted with “Bohart-Adams”, “Yan”, “Belter-Cussler-Hu” and “Clark” models. Such models have been plotted the “breakthrough curves” for contaminant transport along the packed beads. Belter-Cussler-Hu is more suitable model in the description of the outcomes obtained from continuous tests.

Keywords: antibiotic, fixed bed column, alginate, sesban tree leaves, pomegranate peel.

INTRODUCTION

Groundwater, which is essential to both aquatic and terrestrial ecosystems, is considered the most precious and easily accessible freshwater natural resource (Faisal and Ahmed, 2014; Ibreesam and Faisal, 2020). Up to 2 billion people receive drinking water from aquifers, and agricultural regions irrigated by groundwater are responsible of producing forty percent of food in the world (Thiruvengkatachari et al., 2008). Environmental contamination is one of the most important problems resulting from human development in the present century. Groundwater and water bodies may be polluted due to the spillage of industrial wastewater that contains organic chemicals, heavy metals, and radioactive species. Accordingly, the aquatic systems and health of people may be seriously threatened by this pollution (Faisal

et al., 2021; Yang et al., 2017). Pharmaceuticals are well-known organic substances found in water streams that were identified as contaminants in the 1980s (Abed and Faisal, 2023a; Ghattas et al., 2017). The modern community's increased use of these substances to enhance living quality may result in hazardous pollution for ambient environment (Abed and Faisal, 2024; Rivera-Jiménez and Hernández-Maldonado, 2008). Cosmetics, fragrances, antibiotics, sweeteners, agrochemicals, veterinary drugs and pesticides are examples of such contaminants. Tetracycline (TC) and amoxicillin (AMX) are antibiotics that have long-lasting biological and structural activity. These compounds can harm microorganisms or even result in the emergence of new bacterial and viral strains (Faisal et al., 2024b; Tijani et al., 2016). More than one hundred thousand tons of the mentioned antibiotics are annually consumed

in worldwide, according to previous studies (Kummerer, 2003).

Amoxicillin, is semi-synthetic drug belonging to the class of Penicillins from β - lactam antibiotic family that has high stability in water. AMX, which has the molecular formula $C_{16}H_{19}N_3O_5S$, is a white or nearly white powder that is compatible with citrate, phosphate with slight sulfurous odor, and borate buffers as well as available in three different forms: anhydrous, sodium and trihydrate. This antibiotic has lowest solubility for pH range from 4 to 6 (Al-Hashimi et al., 2023, 2021; Hom-sirikamol et al., 2016).

To remove antibiotics from environmental media, a number of treatment approaches have been proposed. As significant technologies, adsorption, membrane separation, oxidation, coagulation, and biological degradation are employed. In the water treatment process, adsorption is flexible, inexpensive, and simple to use (Li et al., 2021; Peng et al., 2016; Shabani and Dinari, 2022; Tkaczyk et al., 2020). Synthesis of efficient materials to obtain suitable remediation of water- chemical compounds is a suitable solution for the contamination problem (Karaman et al., 2022; Karimi-Maleh et al., 2022; Qiu et al., 2022). Since the appearance of the PRB technique in the early 1990s, its long-term performance and capability to retain a wide range of contaminants from groundwater has been thoroughly examined (Abdul-Kareem and Faisal, 2020; Alquzweeni and Faisal, 2020; Faisal et al., 2018; Rashid and Faisal, 2019). Therefore, the PRB technique is introduced as a proper alternative to the traditional “Pump and Treat” approach, especially when the reactive materials of barrier can be prepared from solid wastes discarded to the environment (Qiu et al., 2022).

LDHs are considered a category of ionic lamellar compounds composed of layers having positive charges similar to brucite and interlayer containing solvation molecules and charge compensating anions. The granular structure of such compounds can limit its capacity for sorption because it is led to dense multi-layered stacking. The magnetic biochar can be utilized as immobilized material for loading LDH, thereby high contaminant removal may be achieved (Abed and Faisal, 2023b; Yang et al., 2020).

According to previous studies, the contamination of water resources by effluents containing AMX cannot be denied. To deal with this issue, remediation technologies must be continuously updated. As a result, the production of new

sorbents for PRB allowing for groundwater movement while retaining the chemicals may serve as a sound justification for present investigation. The creation of new reactive material from solid wastes to remediate the AMX-water is the core of present work. This requires the mixing of silver (prepared with pomegranate peels) and iron (extracted with leaves of sesban tree) to form LDH nanoparticles which immobilized as beads using sodium alginate. A set of batch – continuous experiments were conducted to identify the ability of the aforementioned beads and suitable operation conditions in the reclamation of AMX-water.

METHODOLOGY IN THE LABORATORY

Contaminant

To investigate the ability of water reclamation using prepared beads, the AMX antibiotic was chosen in the batch and continuous tests. A 1 L water plus 1000 mg AMX were mixed together to form stock solution of 1000 mg/L which could be diluted to achieve the required concentration. The acidity of the room-temperature stock solution needed to be gradually adjusted by drops of NaOH or HCl as needed. A “UV-visible spectrophotometer” (Varian Cary 100 conc., England) set to 230 nm was used to measure the antibiotic concentration (Ataklti et al., 2016; Wang and Jian, 2015).

Preparation of silver ions

Pomegranate peels were used to help in producing silver ions. The peels were first removed from other components, including fruit, membranes, seeds and they were then washed by “distilled water, DW” as well as air dried for enough time to eliminate any remaining moisture before being ground into tiny bits. Five grams of these fragments were combined with one hundred milliliters of DW, and the mixture needed to be heated to 60 degrees Celsius for fifteen minutes. In the following stage, this combination had to be run through a filter paper with a “0.45 μ m pore size” in order to be used as fresh extract. After dissolving 2.2 g of silver nitrate in 250 ml of DW without illumination, it was heated to 60 °C while being stirred. Lastly, a burette was used to add the 50 ml of pomegranate peel extract drop by drop while stirring 100 ml of deionized water. After adding 50 milliliters of diluted pomegranate peel, the

mixture was stirred. Drops of 0.1 M HCl had to be added to verify the conversion of Ag^+ to Ag^0 ; the appearance of white precipitates meant that the Ag^+ was still present. Consequently, pomegranate peels were added until no white precipitate was seen. The process of extracting silver ions from pomegranate peels is shown in Figure 1.

Preparation of iron ions

The leaves of sesbania tree were washed with DW and; then, they had to be converted to fine powder after being dried for five days to eliminate any remaining moisture. Next, 100 milliliters of DW had to be combined with five grams of sesbania powder. The liquid was heated to 60 °C for fifteen minutes and then had to be passed on the “0.45 μm pore size” filter paper. It was necessary to dissolve 2.16 grams FeCl_3 in 83.3 ml DW at 40 °C with agitation. Thereafter, 50 ml of extract was diluted with DW to 100 ml, then added drop by drop using a burette while being stirred and heated to 40 °C. The process of extracting iron ions from sesbania leaves is described in Figure 1.

Manufacture of Ag/Fe composite

The 100 milliliters of silver solution had to be added to 100 milliliters of iron solution. The resultant mixture was agitated at 250 rpm for 3 h using a magnetic stirrer. After that, the resulting material could be filtered out of the aqueous solution, but it had to remain at 60 °C overnight. Polymer matrix of sodium-alginate (supplied from China having 2.5×10^5 g/mol) was applied to immobilize the silver-iron nanoparticles to obtain the LDH beads. Figure 1 provides an illustration of alginate beads manufacturing process. Three values of pH, specifically around 7, 9 and 11 for mixture were adopted to find its effect on synthesis process for 3 h agitation at 250 rpm. The rise of pH is very important to support the preparation of nanoparticles.

The same process outlined in previous scientific papers was used to produce sodium alginate. Therein, 2-gram sodium-alginate were dissolved in 100 milliliters of DW as part of this procedure. Using a stirrer, the solution was thoroughly mixed for 24 hours at room temperature. Preformed nanoparticles at varying quantities were added to a sodium alginate solution. The 0.1 M CaCl_2 solution, which can be made by dissolving 1 gram of CaCl_2 in 100 milliliters of

DW, had to be mixed with the slurry. This was done using a 10-milliliter syringe to start the polymerization process and produce beads. The 4 mm-diameter beads had to be dried at 105 °C. After an hour of immersion in this solution, the beads were washed with DW and kept for later use at 4 °C in a five mM solution of CaCl_2 (0.278 grams of CaCl_2 dissolved in 500 milliliters of DW). The appropriate parameters for bead preparation, such as the silver/iron ratio, nanoparticle dosage, and pH of solution, were identified using the AMX elimination efficiency as an indicator. The removal efficiency (R) of AMX on the prepared beads is illustrated below:

$$R = \frac{(C_o - C_e)}{C_o} \times 100 \quad (1)$$

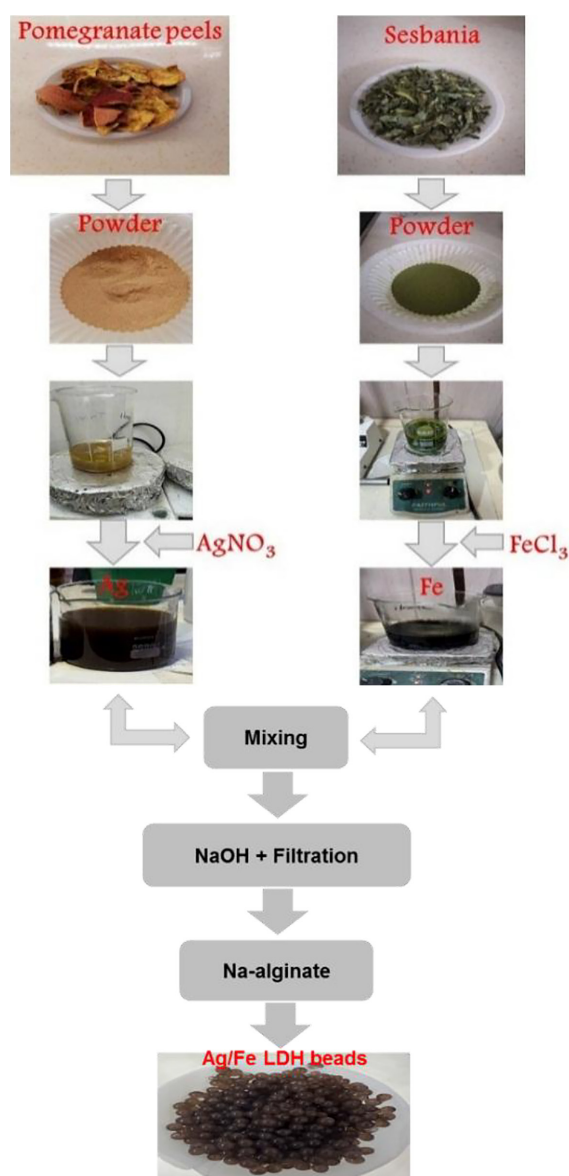


Figure 1. Schematic methodology for preparation of LDH alginate beads

Column tests

A Perspex column supplied with peristaltic pump, water storage tank, tubes and valve represented the components of experimental setup (Fig. 2) used for modeling the migration of AMX dissolved in water. The dimensions of column were inner diameter 2.5 cm, height 50 cm and wall thickness 3 mm. For uniform water movement to match the actual situation in the packed beds, antibiotic migration through the column was considered to be one-dimensional. Only 40 cm Ag/Fe LDH alginate beads were added to the column in order to test its ability in the capture of AMX molecules. To avoid entrapped air, DW at room temperature had to be pumped through the aforementioned bed in the shape illustrated in Figure 2. At saturation state, the AMX-water was pumped to the bed of beads at 1, 2.5, and 5 mL/min with specific hydraulic gradient. The flowrates were selected to obtain the laminar flow in the packed beads (number of Reynold must less than 1) which simulate the situation of groundwater (Delleur, 1999). From Darcy's law, the coefficient of permeability for packed beads is calculated. The P1-P4 were ports positioned at 10–40 cm, respectively. To measure the AMX concentration, samples of water were taken from P1 and P4 at predetermined intervals. The AMX concentrations in the influent for the continuous testing were 50, 100, and 150 mg/L.

MODELING OF COLUMN TESTS OUTPUTS

The C/C_0 versus elapsed time (“breakthrough curves”) could be measured by experiments at specific locations along the one dimensional

packed column and these curves could be simulated by a set of mathematical models. The “breakthrough curve” can be used as an efficient method to design of PRB in field scale. The described curve can be plotted as “S-shaped” for constant continuous influent concentration. The “breakthrough point” is a unique property that can be specified by “breakthrough curve”. This point represents the outlet concentration that satisfied the water purifying objective. Analytical solution can be derived for simple problems to solve the equation of solute transport to plot the breakthrough curves; however, such a solution cannot be developed for complex situations. Therefore, development of empirical approximations and semi analytical solutions with aid of computer were implemented. In comparison with numerical solutions, the application of such tractable and simpler models to describe the contaminant transport in the reactive bed with acceptable accuracy was required (Chu, 2004). Table 1 lists the empirical and theoretical models applied in this study.

RESULTS AND DISCUSSION

Beads manufacturing

Specifying the synthesis parameters of produced beads for sorbing AMX from water was the main goal of the preparation experiments. The Ag to Fe ratio, the amount of nanoparticles, and the initial pH of the water are the main manufacturing parameters adopted in this study. The higher AMX elimination corresponds to the optimal value of each condition.

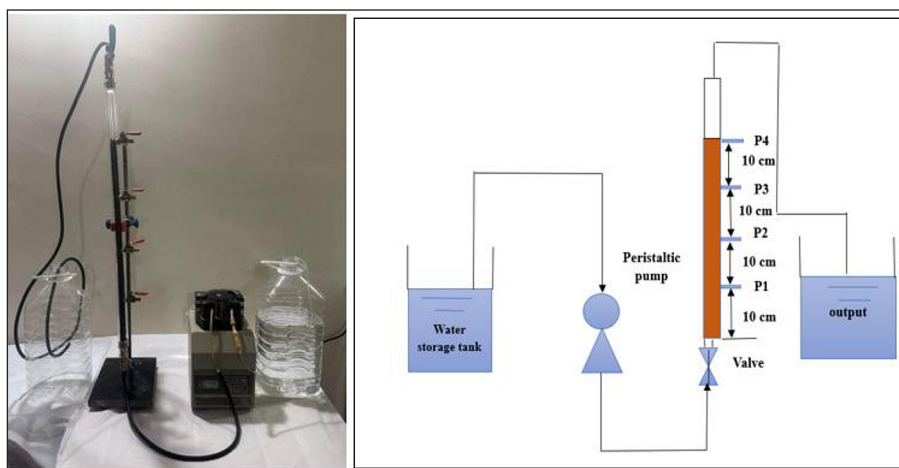


Figure 2. Column set-up for testing the propagation of AMX along the alginate beads

Table 1. Models for formulating of continuous measurements from column tests

Model	Formula	Reference
Bohart-Adams	$\frac{C}{C_o} = \frac{1}{1 + \exp\left(KN_o\frac{z}{U} - KC_o t\right)}$ (2)	(Chatterjee and Schiewer, 2011; Yan et al., 2001)
Yan	$\frac{C}{C_o} = 1 - \frac{1}{1 + \left(\left(0.001 \times C \times Q / q_o M\right) \times t\right)^a}$ (3)	(Kafshgari et al., 2013)
Belter-Cussler-Hu	$\frac{C}{C_o} = 1 + \operatorname{erf}\left[\frac{(t-t_o) \exp\left(-\sigma\left(\frac{t}{t_o}\right)\right)}{\sqrt{2}\sigma t_o}\right]$ (4)	(Chu et al., 2011)
Clark	$\left(\frac{C}{C_o}\right)^{n-1} = \frac{1}{1 + A \cdot e^{-rt}}$ (5)	(Clark, 1987; Medvidovic et al., 2008)

To identify the pH impact on the efficacy of the sorbent synthesis, the pH values were 7, 9 & 11 with 1 for Ag/Fe ratio and 5 g/100 mL dosage of nanoparticles. Using 1 gram of beads per 50 milliliters of solution, 100 mg/L of AMX-water, pH 7, and 250 rotations per minute for three hours, tests successfully identified the removal process. The influence of pH on the ability of sodium alginate to remove AMX during the production process is shown in Table 2. With a value of 35%, the maximum efficiency of removing AMX was noted at pH 9. Because of the increased diameter of the nanoparticle, changes in acidity may result in a notable reduction in percentage of removal. As a result, pH 9 can be adopted during the manufacture process.

An experiment at pH 9 can be applied to evaluate the effect of Ag to Fe ratio in the range (0.5–3) on the creation of beads. Five grams of (Ag/Fe)-LDH nanoparticles were added for every 100 milliliters.

The findings (Table 2) showed that a molar ratio of 0.5 was necessary to attain the greater efficiency (38%). The structural disorder of LDH or the shift in the radius difference between Fe-Ag can result in the efficiency drop when compared to the maximum level (Milagres et al., 2017).

At best pH and molar ratio (i.e. 9 & 0.5 respectively), the effect of nanoparticle mass (1–7 g/100 mL) on bead manufacturing can be examined. The findings are displayed in Table 2. The results provide an explanation for the notable increase in AMX removal efficiency. The efficacy of AMX removal can increase to 58.05% when the quantity of alginate beads is raised from 1 to 7 grams.

Bead characterization

X-ray diffraction (XRD) analysis was utilized for identification the crystalline structure of the materials employed in the production of the

Table 2. Influence of synthesis parameters on the AMX removal percentage using manufactured beads for sorption tests conducted at (3 h, AMX=100 milligram per liter, beads=1 gram per 50 milliliters, 250 rpm, pH 7)

Synthesis parameter	Removal efficiency (%)	Values of other parameters
pH	7	Ag/Fe=1 Ag/Fe-LDH=5 g/100 mL
	9	
	11	
Ag/Fe	0.5	pH=9 Ag/Fe-LDH=5 g/100 mL
	1	
	2	
	3	
Ag/Fe LDH (g/100 mL)	3	pH=9 Ag/Fe=0.5
	4	
	5	
	6	
	7	

present beads. This structure is plotted in Figure 3 for a) Ag, b) Fe, and c) Ag/Fe-LDH. At particular intensities, a number of diffraction reflections (Fig. 3) are discernible, as indicated by 2θ at 13.4, 20.5, 32.3, 43.5, and 45.2. The active sites in charge of removing AMX from water are represented by the reflections. “Joint Committee on Powder Diffraction Standards (JCPDSs)” states that the reflections are corresponding silver-iron nanoparticles that prove the effectiveness of synthesis (Ruan et al., 2011; Szabados et al., 2018).

To determine the functional groups that improved AMX sorption, infrared absorption spectra of produced beads were obtained for both before and after AMX sorption. NAH (amides) and -OH (hydroxyl) groups are present in the particles. The wide peak of the alginate beads indicated a broad and strong absorption band in the 3415–3392 cm^{-1} frequency range. The NAH and OH groups, the stretching of H bond, or the creation of inter-layer molecules of water all contribute to this absorption. The peaks at 851 cm^{-1} show the Ag-OH bending and the Ag-O lattice vibrations. The spectrum signifies the presence of distinctive peaks that range from 1626 to 647 cm^{-1} and are equivalent to the stretching of CO_2 in the generated beads. The bands are the result of the asymmetric and symmetric stretching vibration of the carboxylate (-COO) group. Two weak bands of absorption were also visible in the spectra, originating from the -CAC- and -CAO bonds at 1025 and 1127 cm^{-1} , respectively. Following the AMX sorption process, a noticeable peak is seen at 1053 cm^{-1} , which indicates that the OH

group is vibrating and stretching. Therefore, with the help of the previously described groups, AMX antibiotic can be effectively eliminated (Chen et al., 2018; Faisal et al., 2024a).

The morphological properties of the Fe and Ag elements were shown in Figure 4(a & b). Both elements had a spherical form. Furthermore, as shown in Figure 4(c & d), scanning electron microscopy (SEM) can be used to examine the properties of produced beads both before and after AMX-interaction. Figure 4(c & d) shows that the morphology of the manufactured sorbent is heterogeneous, with rod particles at 200 nm and 200 μm . Also, the surfaces of beads are likewise quite compact and disorganized. Large pores on the surface of the beads seem to permit the sorption of oxyanions. Compared to their alginate bead counterpart, the Ag and Fe-based beads show a fragmented surface, suggesting a lesser degree of mechanical strength. After AMX sorption, sodium alginate exhibits observable morphological alterations in comparison to the beads before sorption.

The Brunauer-Emmett-Teller (BET) determines the specific surface area and total pore volume of the sorbent. The surface areas of the produced beads and silver-iron nanoparticles were 15.21 and 19.52 m^2/g , respectively. The average pore volume of beads was 5.518 cm^3/g , while that of nanoparticles was 6.333 cm^3/g . The “mean pore size” of beads and nanoparticles was calculated using the Barrett-Joyner-Halenda (BJH) method, which yielded values of 0.0163 and 0.0178 nm, respectively.

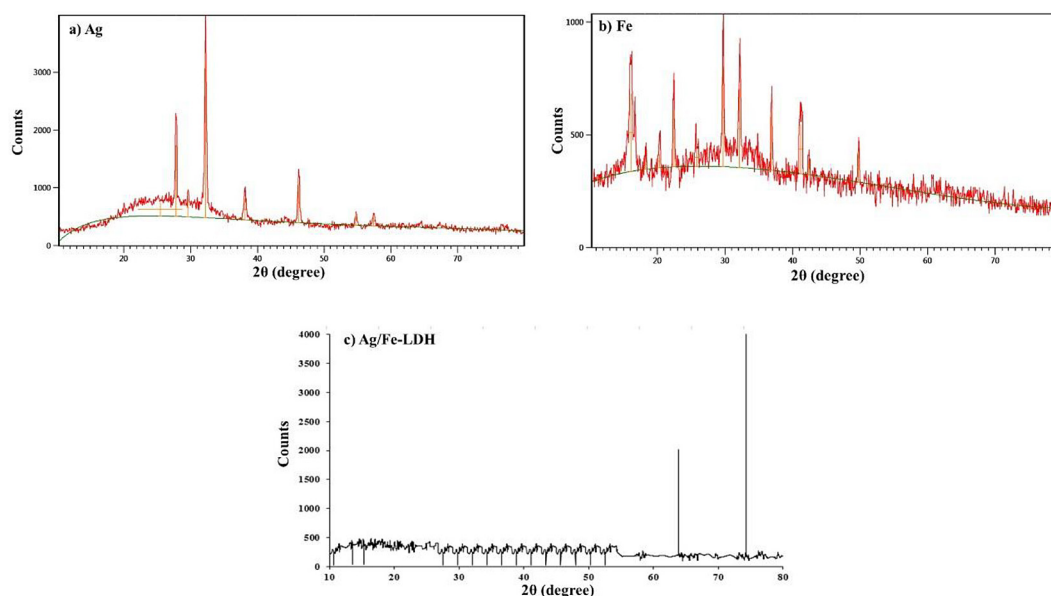


Figure 3. Crystalline structure of alginate beads using XRD analysis

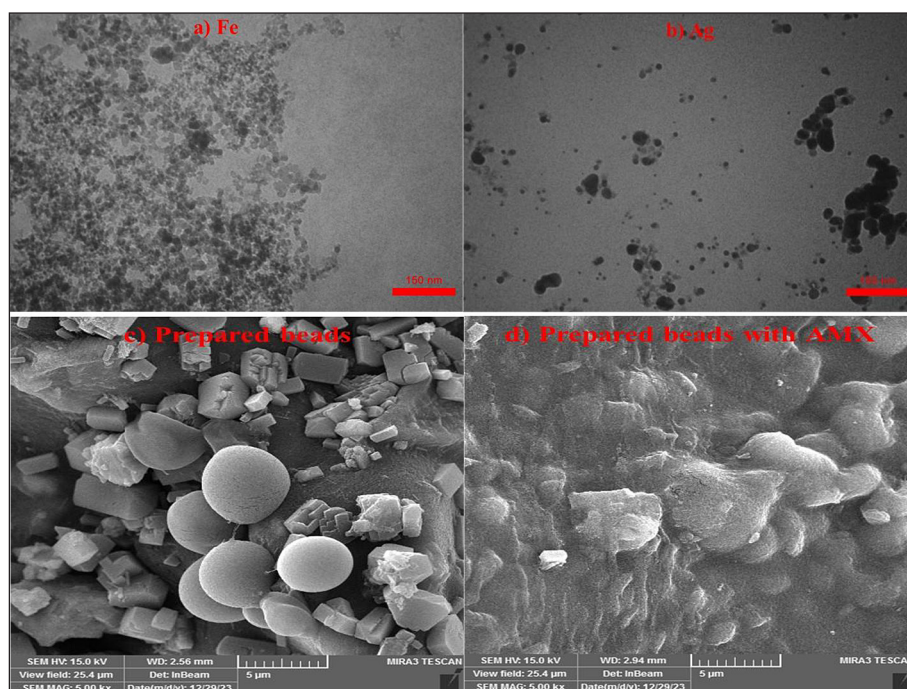


Figure 4. Images of SEM for different materials used in the preparation of beads

Regeneration

A number of experiments were conducted to find whether exhausted beads could be used to remove AMX antibiotic. The performance of adsorption-desorption cycles determines the results of these tests. Using a 0.5 M HCl solution to desorb antibiotic from the exhausted beads is necessary for regeneration. According to the results, the efficiencies for cycles 1, 2, 3, 4, 5, and 6 were 95, 93, 91, 86, 81, and 76%, respectively. It is clear that efficiency decreased with the number of recycling procedures, and after five cycles, over 80% of antibiotics could be removed. The regeneration of exhausted beads is considered a feasible solution to reuse of such sorbent in the extraction of AMX from water, especially in field applications.

Continuous outputs

Migration of AMX through a column setup was tested using prepared beads as PRB. The purpose of monitoring was to find the performance of PRB in the capture of adopted antibiotic from water while keeping the hydraulic conductivity within an acceptable range. The flowrate of water, AMX concentration and bed depth are popular factors that are adopted to explain: (1) variation of C/C_0 for AMX at ports P1 and P4 as function

of time, and (2) simulation of measured breakthrough curves mathematically by Bohart-Adams, Yan, Belter-Cussler-Hu and Clark models.

The effects of C_0 at 50, 100, and 150 mg/L for 1 mL/min on the AMX front propagation for P1 and P4 are clearly seen from the breakthrough curves in Figures 5 and 6. These figures demonstrate how the sorbent will quickly become saturated with pollutant when the influent concentration rises. This caused by the fact that a high gradient of concentration produces a higher driving force for the chemical transfer, which accelerates the exhaustion of adsorption sites (Liao et al., 2013).

The “breakthrough time” that corresponds to 5% C/C_0 for AMX antibiotic may be calculated from the breakthrough graphs. Such time is reflected the “bed longevity” essential to maintain the chemical content in the effluent below the permissible limit regulation. From Figure 5, “breakthrough time” for 10 cm beads (P1) is 2.75 days where flowrate 1 mL/min and C_0 50 mg/L and; this value is considerably lowered to 1.4 days with C_0 150 mg/L. The relation between this time and C_0 for P4 exhibits a similar pattern; at 1 mL/min, longevity can vary from 7 to 3.25 days for C_0 50 and 150 mg/L, respectively.

Effect of flowrate on the C/C_0 front at P1 and P4 for 50, 100 and 150 mg/L are depicted in Figs. 5 and 6. For these figures, the variation in flowrate from 1 to 5 mL/min will speed up the AMX front’s

appearance, shorten the “breakthrough time”, and make the “breakthrough curves” steeper due to contaminant leaving the beads before reaching the equilibrium (Ko et al., 2000). The higher discharge can also desorb a large number of adsorbed molecules from the surface of sorbent especially for weak and reversible bonds. Accordingly, the

“breakthrough time” was decreased due to the rising effluent concentration. For example, the “breakthrough time” can decrease from 7 to 2.5 days if the flowrate is raised from 1 to 5 mL/min for 50 mg/L at P4. The AMX front appearance is significantly delayed by the increased sorbent depth, as shown in Figs. 5 and 6, suggesting that

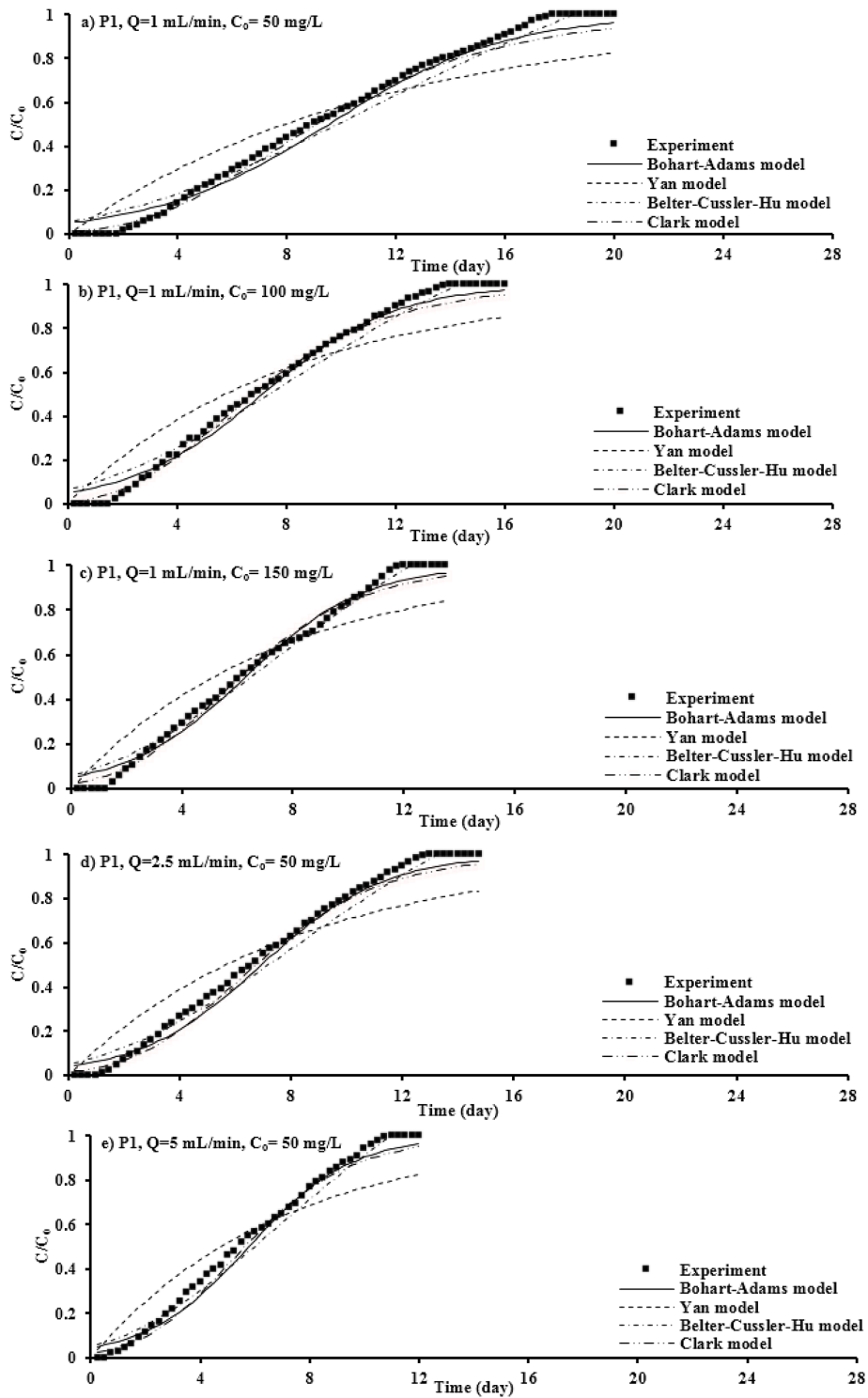


Figure 5. Measured and calculated breakthrough graphs for propagation of AMX front at P1

the bed depth may influence the spread of the contaminant front. When molecules of AMX have enough time to diffuse into the beads pores at the deeper bed, the adsorption process is improved. For 1 mL/min and C_0 50 mg/L, the “breakthrough time” increases from 2.75 to 7 days when beads thickness is changed from 10 to 40 cm; however,

the “saturation time” can be observed to increase from 16.75 to 22 days. It is clear that the higher bed depth will improve the adsorption capacity of such bed for same C_0 due to the raising surface areas at thicker depths. The outcomes proved that the hydraulic conductivity coefficients remain approximately constant at around 2.6×10^{-2} cm/s.

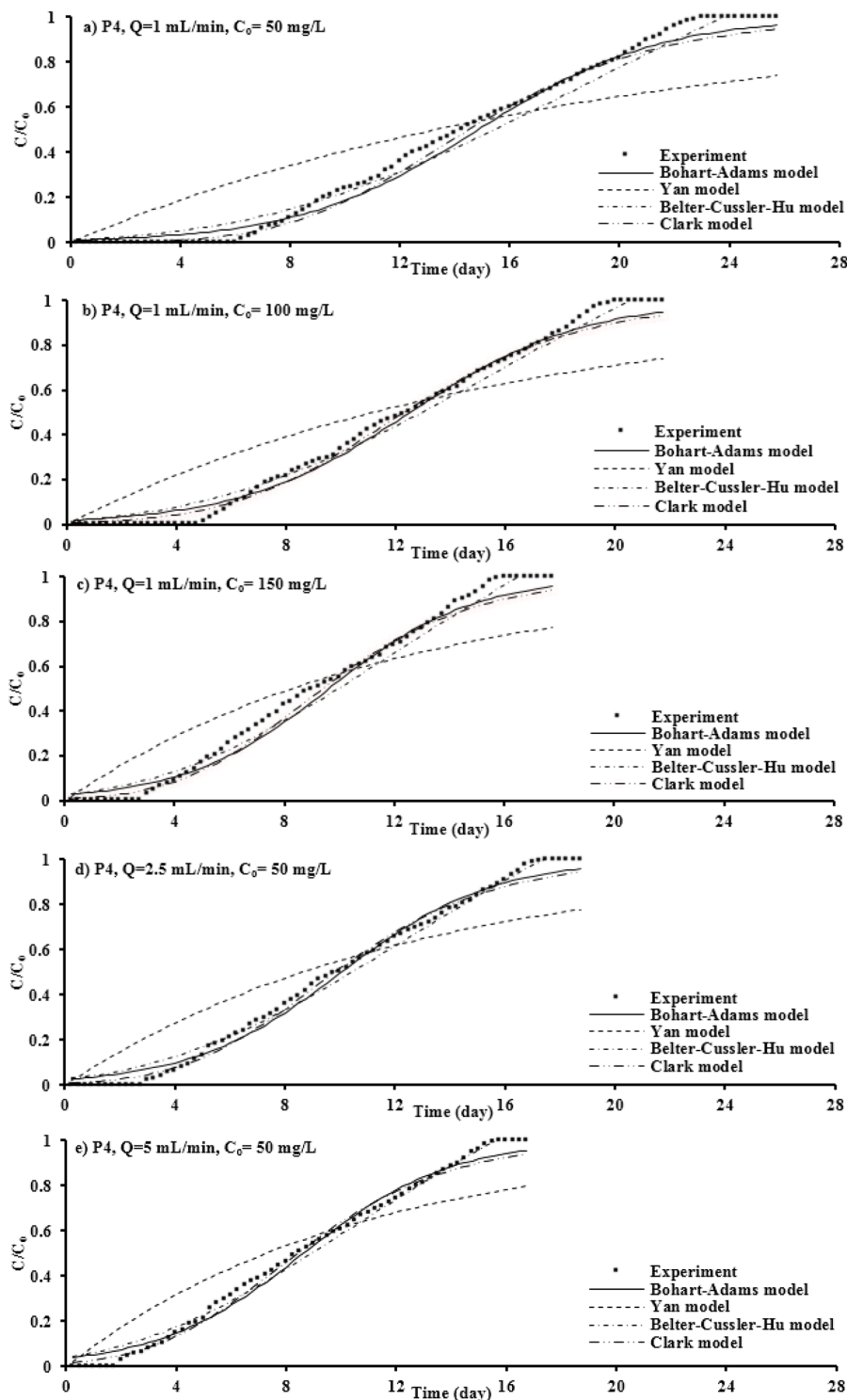


Figure 6. Measured and calculated breakthrough graphs for propagation of AMX front at P4

Table 3. Values of coefficients for models applied to formulate AMX breakthrough curves at P1 and P4 for different C_o at 1 mL/min

Model	Parameter	P1			P4		
		$C_o=50$	100	150	50	100	150
Bohart-Adams	KC_o	0.308	0.411	0.466	0.303	0.319	0.379
	$KN_o \frac{Z}{U}$	2.943	2.933	2.932	4.510	3.991	3.655
	R^2	0.991	0.992	0.988	0.992	0.992	0.988
	SSE	0.153	0.094	0.088	0.168	0.136	0.147
Yan	$\frac{0.001QC}{q_oM}$	50×10^{-5}	8×10^{-5}	15×10^{-5}	7.6×10^{-5}	8.3×10^{-5}	9.7×10^{-5}
	a	171.62	1483.75	848.50	682.68	745.49	859.88
	R^2	0.968	0.969	0.964	0.907	0.912	0.942
	SSE	1.299	1.002	0.779	3.504	2.564	1.655
Belter-Cussler-Hu	t_o	18.546	14.289	12.262	23.781	20.542	16.538
	σ	0.525	0.542	0.527	0.401	0.421	0.450
	R^2	0.981	0.978	0.986	0.983	0.990	0.985
	SSE	0.241	0.204	0.096	0.286	0.153	0.158
Clark	A	0.213	0.262	2.265	6.556	10.013	4.857
	r	0.218	0.295	0.368	0.233	0.263	0.301
	n	1.041	1.049	1.311	1.288	1.479	1.364
	R^2	0.995	0.994	0.989	0.993	0.992	0.990
	SSE	0.140	0.084	0.081	0.167	0.133	0.141

Table 4. Values of coefficients for models applied to formulate AMX breakthrough curves at P1 and P4 for different Q at 50 mg/L

Model	Parameter	P1			P4		
		Q=1	2.5	5	1	2.5	5
Bohart-Adams	KC_o	0.308	0.455	0.531	0.303	0.364	0.378
	$KN_o \frac{Z}{U}$	2.943	3.163	3.074	4.510	3.663	3.258
	R^2	0.991	0.992	0.990	0.992	0.991	0.989
	SSE	0.153	0.096	0.078	0.168	0.094	0.088
Yan	$\frac{0.001QC}{q_oM}$	50×10^{-5}	7.6×10^{-5}	1.6×10^{-5}	7.6×10^{-5}	9.7×10^{-5}	6.3×10^{-5}
	a	171.62	1595.57	780.41	682.68	828.52	1498.88
	R^2	0.968	0.967	0.968	0.907	0.937	0.951
	SSE	1.299	0.958	0.688	3.504	1.691	1.145
Belter-Cussler-Hu	t_o	18.546	13.255	10.987	23.781	17.400	15.633
	σ	0.525	0.513	0.512	0.401	0.454	0.484
	R^2	0.981	0.979	0.983	0.983	0.989	0.990
	SSE	0.241	0.169	0.100	0.286	0.112	0.081
Clark	A	0.213	3.028	3.317	6.556	5.209	3.810
	r	0.218	0.361	0.428	0.233	0.291	0.303
	n	1.041	1.338	1.376	1.288	1.378	1.377
	R^2	0.995	0.994	0.992	0.993	0.992	0.990
	SSE	0.140	0.095	0.074	0.167	0.084	0.078

Accordingly, the pores remain accessible during water movement (contaminant's migration). The proper permeability for PRB is higher than 2.1×10^{-2} cm/s (Bear and Cheng, 2010).

The aforementioned models were fitted with experimental data obtained from continuous testing of the column for the removal of AMX. The breakthrough curves for AMX transport at P1 and P4 along the column can be plotted using these models. Understanding the rate at which the contaminant front will spread along the packed bed depends on the curves of the aforementioned models. The fitted parameters of models (Tables 3 and 4) proved that increasing the bed depth (i.e. alginate beads) greatly enhances the adsorption capacity for AMX.

The parameters of models listed in Tables 3 and 4 were determined from nonlinear fitting by applying Solver Excel spreadsheet tool. The familiar statistical tools (sum of squared errors, SSE, and coefficient of determination, R^2) were calculated to identify the concurrence between measurements and models, consequently, specifying a more adequate model that can be adopted for estimating the breakthrough point on the plotted curves of Figures 5 and 6. The Belter-Cussler-Hu model, with $R^2 > 0.97$ and $SSE < 0.286$, was the appropriate choice for representing the measurements at P1 and P4.

CONCLUSIONS

Ag/Fe-LDH nanoparticles were successfully synthesized through combination of silver ions solution and iron ions solution extracted with aid of solid wastes, specifically peels of pomegranate and leaves of sesban tree, respectively, via precipitation method. The synthesized nanoparticles had to immobilize by Na-alginate to produce an innovative sorbent named Ag/Fe-LDH – sodium alginate beads – PRB for reclamation of contaminated groundwater. This work considered the real application for sustainable development due to use the solid wastes in the production of such bead sorbent. The appropriate parameters for synthesis of beads require Ag to Fe = 0.5, pH = 9 and particles dosage = 7 g/100 mL. The characterization analyses certified that nanoparticles had formed inside the manufactured sorbent and may facilitate the sorption of AMX, particularly when the main component of particles was (Ag/Fe-LDH). The findings for the effectiveness of PRB

to limit AMX migration prove that the lower inlet concentration, lower water flowrate, and higher beads quantity can increase the PRB longevity. Hence, the highest values for breakthrough time and saturation time were equal to 7 and 22 days achieved at lowest flowrate (1 mL/min), concentration (50 mg/L) and higher depth equal to 40 cm. Belter-Cussler-Hu model is an appropriate model for formulating the data of column tests. With an average coefficient of permeability 2.6×10^{-2} cm/s, the results showed that the voids in the packed beds are still capable of transporting polluted water.

REFERENCES

1. Abdul-Kareem, M.B., Faisal, A.A.H., (2020). Permeable reactive barrier of coated sand by iron oxide for treatment of groundwater contaminated with cadmium and copper ions. *Al-Khwarizmi Eng. J.* 16, 47–55. <https://doi.org/10.22153/kej.2020.05.002>
2. Abed, M.F., Faisal, A.A.H., (2023a). Calcium/iron-layered double hydroxides-sodium alginate for removal of tetracycline antibiotic from aqueous solution. *Alexandria Eng. J.* 63, 127–142. <https://doi.org/10.1016/j.aej.2022.07.055>
3. Abed, M.F., Faisal, A.A.H., (2023b). Green synthesis of calcium/iron-layered double hydroxides-sodium alginate nanoadsorbent as reactive barrier for antibiotic amoxicillin removal from groundwater. *Adsorpt. Sci. Technol.* 1–12. <https://doi.org/10.1155/2023/1475278>
4. Al-Hashimi, O., Hashim, K., Loffill, E., Marolt Čebašek, T., Nakouti, I., Faisal, A.A.H., Al-Ansari, N., (2021). A comprehensive review for groundwater contamination and remediation: occurrence, migration and adsorption modelling. *Molecules* 26, 5913. <https://doi.org/10.3390/molecules26195913>
5. Al-Hashimi, O., Hashim, K., Loffill, E., Nakouti, I., Faisal, A.A.H., Čebašek, T.M., (2023). Eco-friendly remediation of tetracycline antibiotic from polluted water using waste-derived surface re-engineered silica sand. *Sci. Rep.* 13, 13148. <https://doi.org/10.1038/s41598-023-37503-4>
6. Alquzweeni, S.S., Faisal, A.A.H., (2020). Removal of lead ions from aqueous solution using granular iron slag byproduct as permeable reactive barrier. *Iraqi J. Agric. Sci.* 51, 723–733.
7. Ataklti, A., Alemu, K., Abebe, B., (2016). Study of the self-association of amoxicillin, thiamine and the hetero-association with biologically active compound chlorgenic acid. *African J. Pharm. Pharmacol.* 10, 393–402. <https://doi.org/10.5897/ajpp2016.4542>

8. Bear, J., Cheng, A.H.-D., (2010). Modeling groundwater flow and contaminant transport. Springer.
9. Chatterjee, A., Schiewer, S., 2011. Biosorption of cadmium(II) ions by citrus peels in a packed bed column: Effect of process parameters and comparison of different breakthrough curve models. *CLEAN - Soil, Air, Water* 39, 874–881. <https://doi.org/10.1002/clen.201000482>
10. Chen, H., Chen, Z., Zhao, G., Zhang, Z., Xu, C., Liu, Y., Chen, J., Zhuang, L., Haya, T., Wang, X., (2018). Enhanced adsorption of U(VI) and 241 Am(III) from wastewater using Ca/Al layered double hydroxide@carbon nanotube composites. *J. Hazard. Mater.* 347, 67–77. <https://doi.org/10.1016/j.jhazmat.2017.12.062>
11. Chu, K., (2004). Improved fixed bed models for metal biosorption. *Chem. Eng. J.* 97, 233–239. [https://doi.org/10.1016/S1385-8947\(03\)00214-6](https://doi.org/10.1016/S1385-8947(03)00214-6)
12. Chu, K.H., Feng, X., Kim, E.Y., Hung, Y.-T., (2011). Biosorption parameter estimation with genetic algorithm. *Water* 3, 177–195. <https://doi.org/10.3390/w3010177>
13. Delleur, J.W., (1999). The handbook of groundwater engineering. *CRC Press. Boca Rat.* 1–974.
14. Faisal, A., and Ahmed, M., (2014). Remediation of groundwater contaminated with copper ions by waste foundry sand permeable barrier. *J. Eng.* 20, 62–77 20, 62–77.
15. Faisal, A.A.H., Mokif, L.A., Hassan, W.H., Al-Zubaidi, R., Al Marri, S., Hashim, K., Khan, M.A., Al-sareji, O.J., (2024a). Continuous and funnel-gate configurations of a permeable reactive barrier for reclamation of groundwater laden with tetracycline: experimental and simulation approaches. *Sci. Rep.* 14, 22907. <https://doi.org/10.1038/s41598-024-73295-x>
16. Faisal, A.A.H., Mokif, L.A., Hassan, W.H., Al-Zubaidi, R., Al Marri, S., Hashim, K., Khan, M.A., Alsareji, O.J., (2024b). Continuous and funnel-gate configurations of a permeable reactive barrier for reclamation of groundwater laden with tetracycline: experimental and simulation approaches. *Sci. Rep.* 14, 22907. <https://doi.org/10.1038/s41598-024-73295-x>
17. Faisal, A.A.H., Shihab, A.H., Naushad, M., Ahamad, T., Sharma, G., Al-Sheetan, K.M., (2021). Green synthesis for novel sorbent of sand coated with (Ca/Al)-layered double hydroxide for the removal of toxic dye from aqueous environment. *J. Environ. Chem. Eng.* 9, 105342. <https://doi.org/10.1016/j.jece.2021.105342>
18. Faisal, A.A.H., Sulaymon, A.H., Khaliefa, Q.M., (2018). A review of permeable reactive barrier as passive sustainable technology for groundwater remediation. *Int. J. Environ. Sci. Technol.* 15, 1123–1138. <https://doi.org/10.1007/s13762-017-1466-0>
19. Ghattas, A.-K., Fischer, F., Wick, A., Ternes, T.A., (2017). Anaerobic biodegradation of (emerging) organic contaminants in the aquatic environment. *Water Res.* 116, 268–295. <https://doi.org/10.1016/j.watres.2017.02.001>
20. Homsirikamol, C., Sunsandee, N., Pancharoen, U., Nootong, K., (2016). Synergistic extraction of amoxicillin from aqueous solution by using binary mixtures of Aliquat 336, D2EHPA and TBP. *Sep. Purif. Technol.* 162, 30–36. <https://doi.org/10.1016/j.seppur.2016.02.003>
21. Ibreesam, M.M., Faisal, A.A.H., (2020). Using cement kiln dust as low permeable barrier for restriction the propagation of cadmium ions towards the water resources. *Iraqi J. Agric. Sci.* 51, 1581–1592. <https://doi.org/10.36103/IJAS.V51I6.1185>
22. Kafshgari, F., Keshtkar, A.R., Mousavian, M.A., (2013). Study of Mo (VI) removal from aqueous solution: application of different mathematical models to continuous biosorption data. *Iranian J. Environ. Health Sci. Eng.* 10, 14. <https://doi.org/10.1186/1735-2746-10-14>
23. Karaman, C., Karaman, O., Show, P.-L., Karimi-Maleh, H., Zare, N., (2022). Congo red dye removal from aqueous environment by cationic surfactant modified-biomass derived carbon: Equilibrium, kinetic, and thermodynamic modeling, and forecasting via artificial neural network approach. *Chemosphere* 290, 133346. <https://doi.org/10.1016/j.chemosphere.2021.133346>
24. Karimi-Maleh, H., Khataee, A., Karimi, F., Baghayeri, M., Fu, L., Rouhi, J., Karaman, C., Karaman, O., Boukherroub, R., (2022). A green and sensitive guanine-based DNA biosensor for idarubicin anticancer monitoring in biological samples: A simple and fast strategy for control of health quality in chemotherapy procedure confirmed by docking investigation. *Chemosphere* 291, 132928. <https://doi.org/10.1016/j.chemosphere.2021.132928>
25. Ko, D.C.K., Porter, J.F., McKay, G., (2000). Optimised correlations for the fixed-bed adsorption of metal ions on bone char. *Chem. Eng. Sci.* 55, 5819–5829. [https://doi.org/10.1016/S0009-2509\(00\)00416-4](https://doi.org/10.1016/S0009-2509(00)00416-4)
26. Kummerer, K., (2003). Significance of antibiotics in the environment. *J. Antimicrob. Chemother.* 52, 5–7. <https://doi.org/10.1093/jac/dkg293>
27. Li, Q., Chen, Z., Wang, H., Yang, H., Wen, T., Wang, S., Hu, B., Wang, X., (2021). Removal of organic compounds by nanoscale zero-valent iron and its composites. *Sci. Total Environ.* 792, 148546. <https://doi.org/10.1016/j.scitotenv.2021.148546>
28. Liao, P., Zhan, Z., Dai, J., Wu, X., Zhang, W., Wang, K., Yuan, S., (2013). Adsorption of tetracycline and chloramphenicol in aqueous solutions by bamboo charcoal: A batch and fixed-bed column

- study. *Chem. Eng. J.* 228, 496–505. <https://doi.org/10.1016/j.ccej.2013.04.118>
29. Marwa F. Abed, Ayad A.H. Faisal, 2024. Na-alginate beads of calcium / iron-layered double hydroxide for treating water contaminated with amoxicillin antibiotic. *Iraqi J. Agric. Sci.* 55, 858–867. <https://doi.org/10.36103/x9f67y59>
 30. Milagres, J.L., Bellato, C.R., Vieira, R.S., Ferreira, S.O., Reis, C., (2017). Preparation and evaluation of the Ca-Al layered double hydroxide for removal of copper(II), nickel(II), zinc(II), chromium(VI) and phosphate from aqueous solutions. *J. Environ. Chem. Eng.* 5, 5469–5480. <https://doi.org/10.1016/j.jece.2017.10.013>
 31. Peng, N., Hu, D., Zeng, J., Li, Y., Liang, L., Chang, C., (2016). Superabsorbent cellulose–clay nanocomposite hydrogels for highly efficient removal of dye in water. *ACS Sustain. Chem. Eng.* 4, 7217–7224. <https://doi.org/10.1021/acssuschemeng.6b02178>
 32. Qiu, M., Liu, L., Ling, Q., Cai, Y., Yu, S., Wang, S., Fu, D., Hu, B., Wang, X., (2022). Biochar for the removal of contaminants from soil and water: a review. *Biochar* 4, 19. <https://doi.org/10.1007/s42773-022-00146-1>
 33. Rashid, H., Faisal, A., (2019). Removal of dissolved trivalent chromium ions from contaminated wastewater using locally available raw scrap iron-aluminum waste. *Al-Khwarizmi Eng. J.* 15, 134–143.
 34. Rivera-Jiménez, S.M., Hernández-Maldonado, A.J., (2008). Nickel(II) grafted MCM-41: A novel sorbent for the removal of Naproxen from water. *Microporous Mesoporous Mater.* 116, 246–252. <https://doi.org/10.1016/j.micromeso.2008.04.009>
 35. Ruan, X., Sun, P., Ouyang, X., Qian, G., (2011). Characteristics and mechanisms of sorption of organic contaminants onto sodium dodecyl sulfate modified Ca-Al layered double hydroxides. *Chinese Sci. Bull.* 56, 3431–3436. <https://doi.org/10.1007/s11434-011-4762-y>
 36. Shabani, S., Dinari, M., (2022). Itaconic acid-modified layered double hydroxide/gellan gum nanocomposites for Congo red adsorption. *Sci. Rep.* 12, 4356. <https://doi.org/10.1038/s41598-022-08414-7>
 37. Szabados, M., Varga, G., Kónya, Z., Kukovecz, Á., Carlson, S., Sipos, P., Pálkó, I., (2018). Ultrasonically-enhanced preparation, characterization of CaFe-layered double hydroxides with various interlayer halide, azide and oxo anions (CO₃²⁻, NO₃⁻, ClO₄⁻). *Ultrason. Sonochem.* 40, 853–860. <https://doi.org/10.1016/j.ultsonch.2017.08.041>
 38. Thiruvenkatachari, R., Vigneswaran, S., Naidu, R., (2008). Permeable reactive barrier for groundwater remediation. *J. Ind. Eng. Chem.* 14, 145–156. <https://doi.org/10.1016/j.jiec.2007.10.001>
 39. Tijani, J.O., Fatoba, O.O., Babajide, O.O., Petrik, L.F., (2016). Pharmaceuticals, endocrine disruptors, personal care products, nanomaterials and perfluorinated pollutants: a review. *Environ. Chem. Lett.* 14, 27–49. <https://doi.org/10.1007/s10311-015-0537-z>
 40. Tkaczyk, A., Mitrowska, K., Posyniak, A., (2020). Synthetic organic dyes as contaminants of the aquatic environment and their implications for ecosystems: A review. *Sci. Total Environ.* 717, 137222. <https://doi.org/10.1016/j.scitotenv.2020.137222>
 41. Wang, C., Jian, J.-J., (2015). Degradation and detoxicity of tetracycline by an enhanced sonolysis. *J. Water Environ. Technol.* 13, 325–334. <https://doi.org/10.2965/jwet.2015.325>
 42. Yan, G., Viraraghavan, T., Chen, M., (2001). A new model for heavy metal removal in a biosorption column. *Adsorpt. Sci. Technol.* 19, 25–43. <https://doi.org/10.1260/0263617011493953>
 43. Yang, C., Wang, L., Yu, Y., Wu, P., Wang, F., Liu, S., Luo, X., (2020). Highly efficient removal of amoxicillin from water by Mg-Al layered double hydroxide/cellulose nanocomposite beads synthesized through in-situ coprecipitation method. *Int. J. Biol. Macromol.* 149, 93–100. <https://doi.org/10.1016/j.ijbiomac.2020.01.096>
 44. Yang, Y., Ok, Y.S., Kim, K.-H., Kwon, E.E., Tsang, Y.F., (2017). Occurrences and removal of pharmaceuticals and personal care products (PPCPs) in drinking water and water/sewage treatment plants: A review. *Sci. Total Environ.* 596–597, 303–320. <https://doi.org/10.1016/j.scitotenv.2017.04.102>